ELSEVIER

Journal of Molecular Catalysis A: Chemical 102 (1995) 163–174

JOURNAL OF MOLECULAR CATALYSIS A: CHEMICAL

Pyridine interaction with a partially hydrogenated MoS_2 modelled surface. A molecular orbital study

Eloy Nouel Rodríguez-Arias [1,a,*], Andrés Eloy Gainza [a], Antonio J. Hernández [a], P. Susana Lobos [a], Fernando Ruette [b]

[a] *Universidad Simón Bolívar, Departamento de Química, Apartado 89000, Caracas 1080-A, Venezuela*

[b] *Centro de Química, Laboratorio de Química Computacional, Instituto Venezolano de Investigaciones Científicas (IVIC), Apartado 21827, Caracas 1020-A, Venezuela*

Received 28 October 1994

Abstract

Chemisorption of pyridine on a partially hydrogenated surface of MoS_2 was modelled by the interaction of a pyridine molecule with a $Mo_3S_8H_2$ cluster. Calculation of total energies, bond orders, diatomic energies, charge transferences and interatomic orbital overlaps was performed by the CNDO/UHF method. Results show a net charge transfer from the pyridine molecule to the Mo adsorption center. The interaction of π-adsorbed pyridine with chemisorbed hydrogen bridged on Mo–Mo positions leads to a partial hydrogenation of the nitrogen compound. A mechanism of pyridine hydrogenation is proposed based on the fact that Mo adsorption centers (vacancies) are pivotal for hydrogen atoms transfer. These results suggest a regioselective hydrogenation.

Keywords: CNDO molecular orbital study; HDN; Hydrogen adsorption; Hydrogenation mechanism; Molybdenum sulphide; Pyridine

1. Introduction

The hydrotreatment of heavy crudes and further treatment of vacuum residues of oil distillation have increased considerably in the past decade [1]. Heavy crudes and vacuum residues contain relatively high percentages of S, N, O, and metals (Ni, V) and make high demands on the catalyst performance. If not removed, N-compounds act as a poison for hydrocracking and reforming catalysts in the later stages of oil refining. The presence of N-compounds leads to a poor stability of the final products that subsequently causes NO_x pollution of the atmosphere. Furthermore, the intensified protection of the environment has led to the sharpening of the norms for S, N, and metal content of petrol products. The hydrodenitrogenation is a process of prime importance for lowering the nitrogen content of low-grade petroleum feedstocks, hence the nitrogen-containing compounds poison the acid catalysts used in petroleum refining [1].

The hydrodenitrogenation (HDN) reaction occurs, generally, by a two-step process: first the

* Corresponding author.

[1] Visiting Fellow, Centro de Química, Laboratorio de Química Computacional, Instituto Venezolano de Investigaciones Científicas (IVIC), Apartado 21827, Caracas 1020-A, Venezuela.

SSDI 1381-1169(95)00079-8

aromatic ring is saturated, followed by removal of nitrogen through C–N bond cleavage. Details of the HDN mechanism have not been clearly established. It is well known that hydrodenitrogenation of aromatic nitrogen-containing heterocyclic compounds requires catalysts with a high hydrogen activity [1–4]. Generally, these reactions are carried out at 300–1500 psig hydrogen and 290–450°C [5–7].

In this paper we study the interaction of a pyridine molecule adsorbed on a hydrogenated MoS_2 model surface. Pyridine is an excellent model molecule for N-compounds present in petroleum feedstocks. The coordination studies of this molecule on semiconductor and metal surfaces, involve both π and N lone-pair electrons in the surface chemical bond [8](a–c), which will play an important role in hydrodenitrogenation reactions (HDN) [8](d,e). As a result different orientations of the pyridine ring plane with respect to the surface plane are conceivable: parallel, perpendicular and tilted. Indeed, examples for all three adsorption geometries have been reported in the literature [9–23]. For example on Cu(110) [10], Pt(110) [11], Pt(111) [9–13], and on Ir(111) [14] the pyridine ring orientation for saturation adsorption conditions is approximately perpendicular to the metal surfaces, whereas on Ag(111) [14,15], Ni(100) [16], and on Pt(110) [12] a parallel orientation has been derived from various experimental techniques for low coverages. On Pt(110) [12], Ag(111) [14,15], and on Ni(100) [16] a phase transition from parallel to perpendicular or inclined has been reported as a function of pyridine surface coverage.

The purpose of this paper is to study the adsorption of pyridine in different bonding modes and on different sites of the MoS_2 surface, which is represented in this work by a partially hydrogenated $Mo_3S_8H_2$ model cluster. Here, the CNDO/UHF method is used as a qualitative tool for analyzing surface–adsorbate interactions. As far as we know, there are no HDN calculations of pyridine on partially hydrogenated MoS_2 reported in literature. Results were interpreted in terms of the relative stability of adsorption on different active sites, bonding modes, activation of C–C, C–H, and C–N bonds, Mo–pyridine bonding interactions, and net charge transfers. In a recent publication [24] we have studied the pyridine adsorption on a MoS_2 modelled surface (Mo_3S_8) using the same semi-empirical method (CNDO/UHF) and we obtained the following conclusions: (a) The activation of C–N and C–C bonds in pyridine is more pronounced in π-adsorption than in σ-adsorption. (b) The electron transfer occurs from pyridine to Mo_3S_8 cluster. This transfer correlates with the stability of adsorption structures, i.e. more stable systems correspond to more withdrawing of electronic charge from the pyridine to the MoS_2 surface model. (c) Interaction between the pyridine and several Mo atoms is observed in the one-center π and σ-bridge adsorption modes. In these cases, the formation of agostic C–H → Mo bonds of the hydrocarbon with the metal center is also observed.

2. Computational details and surface model

As in previous publication [24], the method employed here was a modified version [25,26] of CNDO/UHF [27] from the GEOMO molecular package [28]. This method and the parameters used have given relatively good results for calculations in other systems that contain Mo–C and Mo–S bonds; for example, $Mo(CO)_6$ (the Mo–CO distance of 2.00 Å compare with the experimental value of 2.07 Å and good interpretation of the photoelectron spectra (PES) is obtained) [29](a) and $Mo(SMe)_4$ (very reasonable values of Mo–S distances (2.31 Å as compare with the experimental analogue ($Mo(St\text{-}Bu)_4$) of 2.24 Å) [29](b).

In this work the partially hydrogenated surface was represented by a $H_2Mo_3S_8$ model cluster in which the pyridine molecule will be adsorbed at vacancies located on a Mo atom. Geometries of the cluster and pyridine were taken from literature [30,31]. Atomic parameters are the same as in previous calculations [29](a), [32].

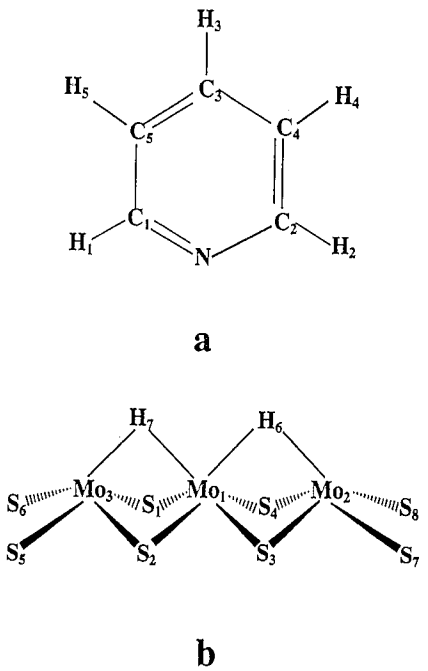

Fig. 1. Structures of (a) pyridine and (b) $Mo_3S_8H_2$.

In order to analyze bonding interactions between the pyridine and the hydrogenated surface, Mulliken bond orders (MBO), diatomic energies (DE), overlap and orbital coefficients of interacting atoms, and the net charge transferred were evaluated. The results of non-hydrogenated surface [24] and isolated systems were included, for comparison.

The surface model consists of a cluster that simulates (see Fig. 1b) the $\bar{1}010$ surface of MoS_2 [33] (d–g), in which the monocoordinated sulfur atoms have been removed by hydrogen treatment. This is in agreement with the experimental work of Wambeke et al. [33] (d). These authors proposed that the mono-coordinated sulfur atoms of the MoS_2/γ-Al_2O_3 catalyst are eliminated at temperatures lower than 473 K. The active site was taken with a formal Mo^{IV} oxidation state located at the center of our trimetallic cluster. Diemann et al. [34] (c) suggest on MoS_2-like crystallites the formation of strongly coordinative unsaturated

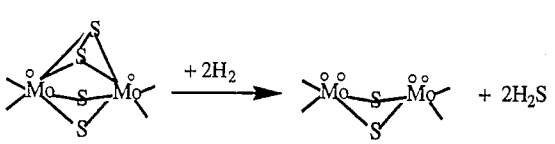

Scheme 1.

activated sites after a pretreatment with hydrogen (Scheme 1). These sites exhibit two vacancies on each Mo atom as in our model. Similar sites have been presented by Hayden and Dumesic's model [34] (d), these are located on the edges of MoS_2 slabs vertically anchored on a surface of γ-Al_2O_3.

It is worth mentioning at this point that a single MoS_2 layer represents a reasonable model for this catalyst because the electronic inter-layer interaction is relative weak. For this reason, we have selected a row of Mo atoms in the $\bar{1}010$ plane that represent the shortest Mo–Mo distance possible. In any other case, Mo atoms are separated by at least three bonds (Mo–S...S–Mo). In fact, this has been found in experimental work on synthesized molybdenum sulphur clusters, which have been employed as precursors of HDS catalysts [34] b and as molecular models of MoS_2 [34] (a).

3. Results and discussion

With the purpose of studying the adsorption of pyridine on the $H_2Mo_3S_8$ cluster, we have carried out calculations of electronic and geometrical properties separately for the pyridine molecule and for the $Mo_3S_8H_2$ cluster shown in Fig. 1a and Fig. 1b, respectively, and for the composite pyridine–$Mo_3S_8H_2$ systems, in three different adsorption modes, as depicted in Fig. 2a–c. The appropriate bond length and bond angles of the two hydrogen atoms adsorbed on the Mo_3S_8 cluster were selected after several optimization calculations, where the total energy of several structures were evaluated for both H atoms adsorbed on sulphur atoms at the edges (S_7 and S_8 in Fig. 1b), one H atom on a Mo_2 and the other on a S_7 atom, and both on Mo atoms (Mo_2 and Mo_3 in Fig. 1b). Calculations were carried out using the Mo–H (1.695 Å) and the S–H (1.34 Å) experimental bond distances from Cp_2MoH_2 [35] and from H_2S [36], respectively. Optimization of the Mo–Mo–H and Mo–S–H angles leads to the conclusion that adsorption of H atoms on MoS_2 is more stable at the bridge Mo–Mo position.

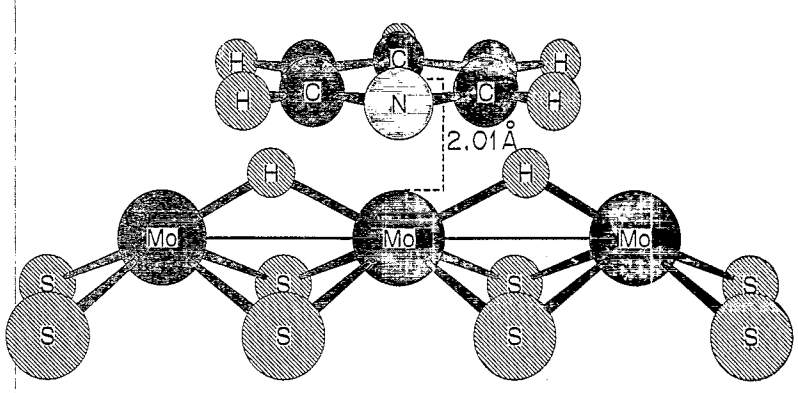

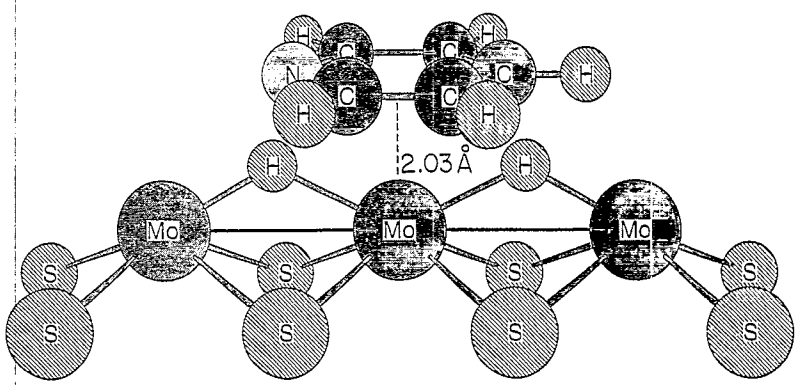

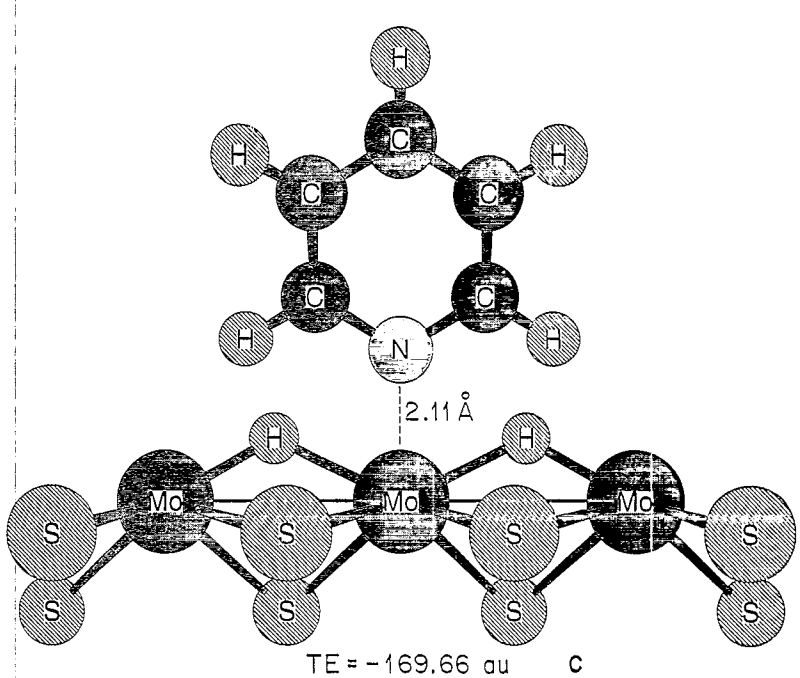

Fig. 2. Pyridine–$Mo_3S_8H_2$ systems, (a) I (b) II, in π-coordinate modes and (c) III, in σ-coordinate mode.

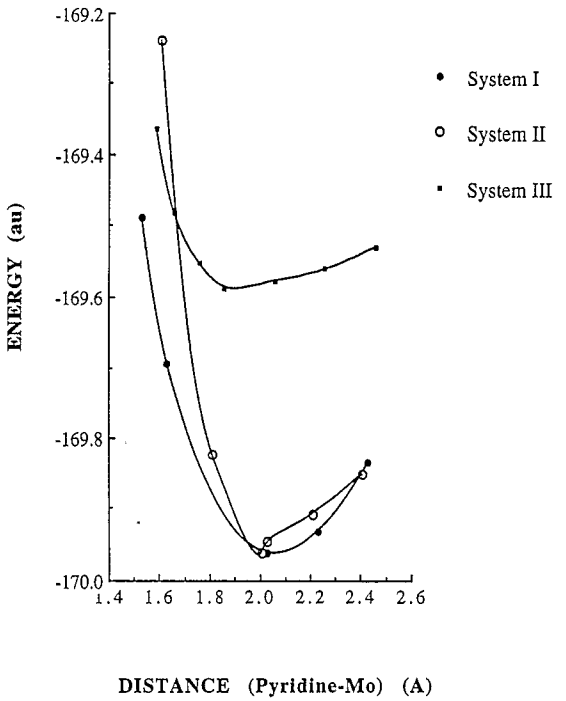

Fig. 3. Potential energy curves for the interaction of pyridine with the Mo_1 center of the $Mo_3S_8H_2$ cluster, for systems I–III (Fig. 2).

The choice of this $Mo_3S_8H_2$ model cluster depicted in Fig. 1b, can be additionally justified by several reasons: (i) Once the vacancy sites are formed (i.e. the surface face $\bar{1}010$ is clean of S atoms), the low-coordinated Mo atoms are able to adsorb hydrogen. (ii) The highest adsorption energy for hydrogen atoms on MoS_2 occurs on Mo sites as reported by the theoretical results of Anderson et al. [37]. (iii) Our model represents a geometrical structure in which adsorption of pyridine results in pyridine–H–Mo distances, which allow bonding interactions; this is not the case for adsorption on S_7 and S_8 in which H atoms are too far away from the pyridine. (iv) There are structurally characterized Mo-complexes containing sulfur ligands and hydrogen bonds to the molybdenum center [38].

As suggested in the literature [1](d), the π- and σ-adsorption modes, as well as the adsorption on one-center sites, were considered in the present study. In all these three adsorption modes, called here systems I, II, and III, respectively, the pyridine molecule approached the $Mo_3S_8H_2$ cluster on top of the Mo_1 atom. Fig. 3 shows the interaction energy of systems I–III as a function of the distance between the pyridine and the Mo_1 atom. The shape of the interaction curves in Fig. 3 indicates a minimum in the interaction for all three cases. This minimum approach of pyridine with respect to the Mo_1 atom for systems I–III, 2.01 Å, 2.03 Å, and 2.11 Å, respectively, are used in the pyridine–$Mo_3S_8H_2$ structures shown in Fig. 2a–c.

Before analyzing in detail the adsorption modes studied in the present work, we must clarify that several spin multiplets were examined in our CNDO/UHF calculations, in all cases the quintuplet state was found to be the most stable. Total binding energies are not used in our analysis because CNDO poorly reproduces dissociation energies for Mo systems, and therefore, scaling with respect to experimental data is required [31]. However, important qualitative information can be obtained from the relative energy stability among systems of similar composition, by comparing their total energies.

3.1. System I

The system I depicted in Fig. 2a, represents the most stable adsorption mode found in the present study. The Mulliken bond orders (MBO) and diatomic energies (DE) of the pyridine molecule adsorbed in a π-mode on $Mo_3S_8H_2$ are presented in Table 1, where we have shown properties for only one symmetry equivalent atom. The corresponding values for the isolated systems (pyridine and $Mo_3S_8H_2$) are also shown in Table 1 for comparison reasons. These MBO and DE values reveal that pyridine is mainly stabilized by coordinative interactions between the Mo_1 surface atom and the pyridine ring atoms (see large values of MBO and DE for the Mo_1–N, Mo_1–C_1, ..., Mo_1–C_5 bonds in Table 1). Nevertheless, these interactions are weaker as compared to the case of the Mo_3S_8–pyridine system, as can be seen from the corresponding values in brackets in Table 1 (these were taken directly from previous work on the interaction of the pyridine with the Mo_3S_8 cluster [24]). This agrees with the fact that the equilibrium bond distance in the pyridine–Mo_3S_8

Table 1
Bonding properties of the system I ($Mo_3S_8H_2$–C_5H_5N) shown in Fig. 2a. Values in parentheses ( ) correspond to isolated systems ($Mo_3S_8H_2$ and pyridine). Values in brackets [ ] are for the Mo_3S_8 system with pyridine interactions. For atom labels, see Fig. 1

Bond	MBO	DE (au)
$Mo_3S_8H_2$–pyridine		
Mo_1–N	0.352 [0.475]	−0.165 [−0.229]
Mo_1–C_1, C_2	0.405 [0.612]	−0.200 [−0.287]
Mo_1–C_3	0.491 [0.613]	−0.241 [−0.287]
Mo_1–C_4, C_5	0.400 [0.607]	−0.185 [−0.287]
Mo_2–C_2, Mo_3–C_1	0.207 [0.314]	−0.116 [−0.170]
Mo_3–C_5, Mo_2–C_4	0.221 [0.336]	−0.121 [−0.172]
Mo_3–H_1, Mo_2–H_2	0.134 [0.186]	−0.044 [−0.056]
Mo_3–H_5, Mo_2–H_4	0.152 [0.214]	−0.051 [−0.065]
H_7–C_1, H_6–C_2	0.335	−0.147
H_6, H_7–N	0.006	−0.004
H_6, H_7–C_3	0.009	−0.005
H_7–C_5, H_6–C_4	0.349	−0.192
Pyridine		
C_1, C_2–N	1.610 (1.691)	−1.255 (−1.348)
C_1–C_5, C_2–C_4	1.750 (1.934)	−1.212 (−1.411)
C_3–C_4, C_5	1.820 (1.914)	−1.283 (−1.389)
$Mo_3S_8H_2$		
Mo_1–H_6, H_7	0.394 (0.670)	−0.170 (−0.224)
Mo_3–H_7, Mo_2–H_6	0.535 (0.818)	−0.156 (−0.241)
Mo_1–Mo_2, Mo_3	0.672 (0.841)	−0.100 (−0.195)

system (measured from the center of mass of the pyridine molecule to the Mo_1 the center of Mo_3S_8) is shorter (1.81 Å) as compared to the $Mo_3S_8H_2$–pyridine system (2.03 Å) [24].

We also mention the following important bonding properties of the interaction of the pyridine with the cluster Mo_3S_8 [24]: (i) Carbon atoms of pyridine display noteworthy interactions with Mo_2 and Mo_3 atoms, as shown by the values of MBO and DE for Mo_2–C_2, Mo_2–C_4, Mo_3–C_5, and Mo_3–C_1 bonds. (ii) Pyridine hydrogens (H_1, H_2, H_4, and H_5) have bonding interactions mainly with the terminal Mo atoms (Mo_2 and Mo_3), as can be inferred from the MBO and DE values shown for the Mo_2–H_2, Mo_2–H_4, Mo_3–H_1, and Mo_3–H_5 bonds in Table 1. (iii) The presence of adsorbed hydrogens (H_6 and H_7) allows relatively important bonding interactions between pyridine C atoms and surface H atoms, as shown by the larger MBO and DE entries for the H_7–C_1, H_6–C_2, H_7–C_5, and H_6–C_4 bonds, as compared to the H_6, H_7–C_3 and H_6, H_7–N bonds in Table 1. This last feature may indicate that H_s atoms are able to hydrogenate the two C–C double bonds in the aromatic system, with the possible formation of a 2,5-dihydropyridyne compound (C_5H_7N). (iv) The interaction of pyridine with the hydrogenated surface induces moderate changes in the bonding structure of the pyridine molecule. In fact a comparison of the MBO and DE values, shown in Table 1 for the $Mo_3S_8H_2$–pyridine system and for the isolated pyridine molecule, evidences that C_1, C_2–N, C_3–C_4, C_5, C_2–C_4 and C_1–C_5 bonds are weakened in going from the isolated pyridine molecule to the chemisorbed pyridine system. This effect is explained in terms of the formation of bonds between the pyridine carbon atoms C_i ($i=1, 2, 4, 5$) and the surface hydrogens H_s ($s=6, 7$). (v) Finally, the pyridine chemisorption largely weakens the cluster structure, i.e. the MBO and DE values of the Mo_i–H_s ($i=1, 2, 3$; $s=6, 7$) and Mo–Mo bonds (shown in the last three rows of Table 1) decrease in going from the cluster–pyridine to the isolated cluster system.

The relatively strong interaction between the ring atoms of pyridine and the Mo_1 atom is confirmed by the values of overlap integrals between C and N orbitals and Mo_1 ones, see Table 2. There, the most important interactions were selected according to the overlap values. For example, the overlap between 2s orbitals of C with 5s and 5 p_z orbitals of the Mo_1 atom are 0.29 and 0.37, respectively. In addition, the pair coefficients for different molecular orbitals are of significant magnitude (between 0.12 to 0.34). A schematic picture of these interactions is presented in Fig. 4.

The interaction of pyridine with other Mo atoms (Mo_2 and Mo_3) can be understood also in terms of overlap and molecular orbital coefficients; see values of 0.21–0.14 for the overlap, and atomic molecular coefficients between 0.33 and 0.10. The overlap between adjacent Mo atoms and the pyridine molecule can be explained in terms of molecular dimensions. For example, the Mo diameter is about 3.04 Å [39] while the internuclear distance Mo_1–Mo_2 is 3.15 Å and the sum of the

Table 2
Overlaps, and atomic coefficients of the interaction of pyridine (N, C_1 and H_p atoms) with $Mo_3S_8H_2$ (system I) surface atoms (Mo_1, Mo_3, H_6, and H_7 atoms)

Orbital coupling	Overlap	Pairs of atomic orbital coefficients (a_x,a_y) (x=Mo_1, Mo_3, H_6, H_7) (y=N, C_1, C_3, H_p)
C and N interactions with Mo_1		
$5s(Mo_1)$–$2s(C_1)$	0.29	(−0.22, −0.34) (−0.24, 0.13)
$5p_x(Mo_1)$–$2s(C_1)$	0.21	(0.26, 0.33) (0.27, −0.15)
$5p_z(Mo_1)$–$2s(C_1)$	0.37	(0.22, 0.34) (0.12, 0.13)
$5s(Mo_1)$–$2s(C_3)$	0.29	(−0.22, −0.30) (0.18, −0.29) (−0.24, 0.22) (0.12, −0.17)
$5s(Mo_1)$–$2p_y(C_3)$	0.25	(−0.22, 0.16) (−0.24, −0.21) (0.12, −0.31)
$5p_z(Mo_1)$–$2s(C_3)$	0.36	(−0.22, −0.30) (0.12, −0.22)
$5s(Mo_1)$–$2s(N)$	0.23	(−0.22, −0.31) (0.18, −0.18) (−0.24, 0.27) (*0.12, −0.24*) (*0.12, 0.24*)
$5p_y(Mo_1)$–$2s(N)$	−0.21	(−0.21, 0.52) (−0.23, −0.12) (0.14, −0.14)
$5p_z(Mo_1)$–$2s(N)$	0.30	(0.22, 0.31) (0.12, −0.28)
C interactions with an adjacent Mo atom (Mo_2)		
$5s(Mo_2)$–$2s(C_2)$	0.20	(−0.13, −0.33) (−0.10, 0.12) (−0.21, 0.15)
$5p_x(Mo_2)$–$2s(C_2)$	0.21	(−0.11, −0.33)
$5p_x(Mo_2)$–$2p_z(C_2)$	−0.14	(0.12, −0.13) (−0.19, −0.12)
$5p_z(Mo_2)$–$2s(C_2)$	0.21	(0.10, 0.12) (0.15, 0.15)
$5p_z(Mo_2)$–$2p_x(C_2)$	−0.14	(0.11, −0.17) (0.10, −0.11)
H–pyridine interactions with Mo_1 and Mo_2		
$5s(Mo_1)$–$1s(H_{1-5})$	0.14	(*0.21, 0.21*) (−0.14, −0.23) (0.14, 0.23)
$5p_x(Mo_1)$–$1s(H_{2,5})$	−0.15	(0.23, 0.15) (−0.23, −0.15)
$5p_x(Mo_1)$–$1s(H_{1,4})$	0.15	(0.23, 0.15) (−0.23, −0.15)
$5p_y(Mo_1)$–$1s(H_3)$	0.16	(0.23, 0.15) (−0.23, −0.15)
$5p_z(Mo_1)$–$1s(H_{1,2,4,5})$	0.14	(0.23, 0.15) (−0.23, −0.15)
$5s(Mo_2)$–$1s(H_{2,5})$	0.24	(0.13, 0.17) (0.14, 0.14)
$5p_x(Mo_2)$–$1s(H_{2,5})$	0.14	(−0.11, −0.17) (0.12, 0.14)
$5p_y(Mo_2)$-$1s(H_{2,5})$	±0.17	(−0.11, 0.15)
$5p_z(Mo_2)$–$1s(H_{2,5})$	0.27	(−0.11, −0.19)
H_6 and H_7 interactions with pyridine		
$2s(C_1)$–$1s(H_7)$	0.32	(−0.34, −0.14) (0.33, 0.22) (*0.12, −0.19*)
$2s(C_2)$–$1s(H_6)$	0.32	(−0.34, −0.14) (−0.33, −0.22) (*0.12, 0.19*)
$2s(C_5)$–$1s(H_6)$	0.33	(−0.33, −0.14) (−0.35, −0.22) (*−0.11, 0.19*)
$2s(C_4)$–$1s(H_7)$	0.33	(−0.33, −0.14) (0.35, 0.22) (*0.11, −0.19*)

pyridine width (C_1–C_2 distance of 2.29 Å) with the C orbital radii (1.04 Å) add up 3.33 Å. A schematic representation of the molecular dimensions and the Mo_2 orbital interactions with the ring atoms of pyridine molecule are depicted in Fig. 5.

The pyridine hydrogens (H_p) display multiple interactions with Mo atoms, as shown in Fig. 6. There, the H_p–Mo interactions are divided into s–s (Fig. 6a) and s–p (Fig. 6b) for a clearer presentation. The values of overlap shown in Table 2 indicate that the most important interactions occur with adjacent Mo atoms. For example, $5p_z(Mo_2)$–$1s(H_{2,5})$ and $5s(Mo_2)$–$1s(H_{2,5})$ interactions show the highest overlap. These interactions are important because increase the possibility of C–H_p activation, favoring then the transfer of surface hydrogens (H_s) from the catalyst to the pyridine with the partial formation of new C–H_s bonds

One of the most important interactions between the pyridine and the hydrogenated Mo–S surface occurs with the H_s atoms adsorbed on Mo atoms (Fig. 7). The last rows of Table 2 show one of the highest overlaps (0.33–0.32). In addition, there are relative high atomic orbital coefficients ($a_{2s(C4)} = 0.33$, and $a_{1s(H7)} = 0.22$) in a molecular orbital in which the $2s(C_4)$–$1s(H_7)$ and $2s(C_5)$–$1s(H_6)$ interactions are relevant. These interactions seem to indicate that a hydrogenation of the pyridine molecule adsorbed in the π-mode is possible.

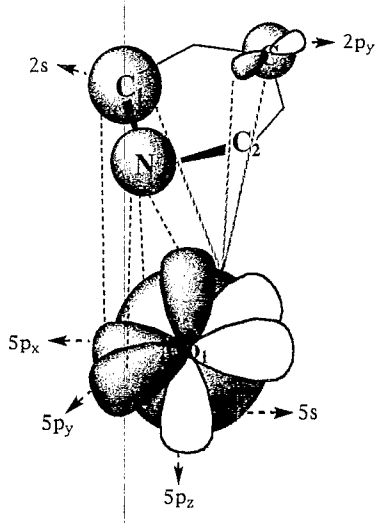

Fig. 4. Schematic representation of atomic orbital interactions between the active site Mo_1 of $Mo_3S_8H_2$ and some pyridine atoms (N, C_1, and C_3) in the system I.

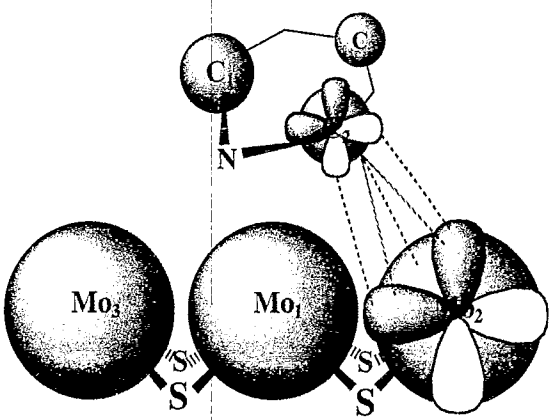

Fig. 5. Orbital interactions between the ring atoms of pyridine molecule (C_2) and Mo_2 center of the $Mo_3S_8H_2$ cluster.

The direct participation of the d orbitals is small and therefore, they are not shown in Table 2. The only important interaction ($4d_{xz}(Mo_1)$–$2p_z(C_3)$) presents an overlap value of 0.10 and orbital coefficients of −0.25 and 0.29. This fact may be due to a longer pyridine–$Mo_3S_8H_2$ bond distance (2.01 Å) than in the case of non-hydrogenated system (1.81 Å) [24].

3.2. System II

Fig. 2b represents the second most stable π-adsorption mode found in the present work. Here, the nitrogen and C_3 atoms are parallel to the molybdenum surface atoms. System II is slightly less stable than system I, and it corresponds to a

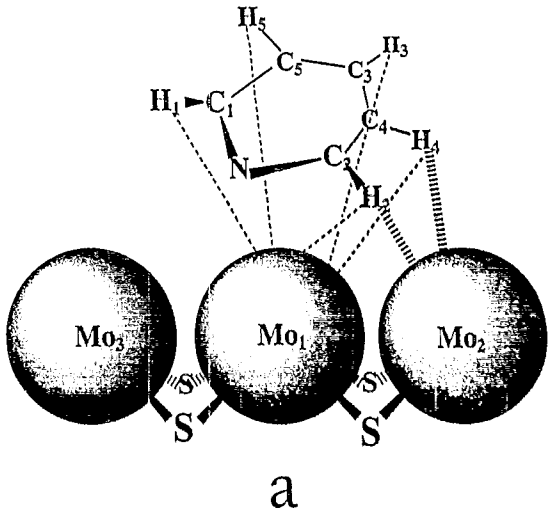

a

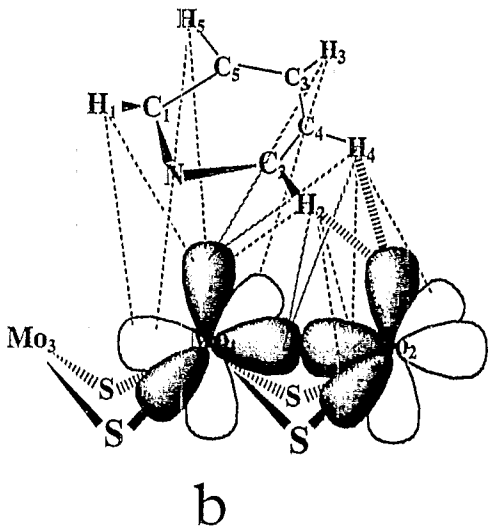

b

Fig. 6. Orbital interactions of pyridine hydrogens with Mo_1 and Mo_2 atoms of the $Mo_3S_8H_2$ cluster. (a) s–s interactions. (b) s–p interactions.

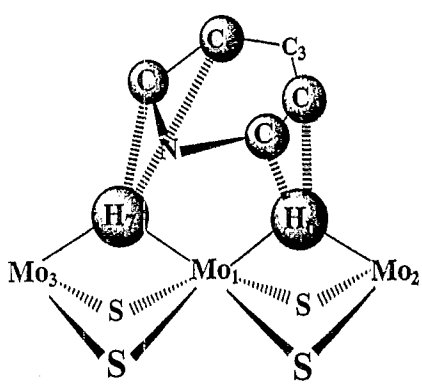

Fig. 7. Orbital interactions between the pyridine molecule and H_s atoms adsorbed on Mo atoms.

Table 3
Bonding properties of the system II ($Mo_3S_8H_2$–C_5H_5N) shown in Fig. 2b. Values in parentheses correspond to isolated systems ($Mo_3S_8H_2$ and pyridine). Values in brackets represent the interactions of Mo_3S_8 system with pyridine. For atom labels, see Fig. 1

Bond	MBO	DE (au)
$Mo_3S_8H_2$–pyridine		
Mo_1-N	0.270 [0.449]	−0.111 [−0.221]
Mo_1–C_1, C_2	0.503 [0.628]	−0.251 [−0.293]
Mo_1–C_3	0.405 [0.586]	−0.187 [−0.279]
Mo_1–C_4, C_5	0.499 [0.622]	−0.239 [−0.283]
Mo_2–N	0.302 [0.414]	−0.124 [−0.222]
Mo_3–C_3	0.390 [0.511]	−0.204 [−0.258]
Mo_3–H_3	0.299 [0.421]	−0.082 [−0.106]
H_7–C_1	0.006	−0.007
H_6–C_2, H_7–C_5	0.040	−0.004
H_6–N	0.707	−0.598
H_7–C_3	0.779	−0.657
Pyridine		
C_1, C_2–N	1.498 (1.691)	−1.112 (−1.348)
C_1–C_5	1.928 (1.934)	−1.418.(−1.411)
C_3–C_5	1.691 (1.914)	−1.149 (−1.389)
C_3–H_3	1.246 (1.363)	−0.641 (−0.748)
$Mo_3S_8H_2$		
Mo_1–H_6, H_7	0.340 (0.670)	−0.130 (−0.224)
Mo_3–H_7, Mo_2-H_6	0.442 (0.818)	−0.097 (−0.241)
Mo_1–Mo_2, Mo_3	0.659 (0.841)	−0.104 (−0.195)

rotamer of the previous system. The calculated MBO and DE values for $Mo_3S_8H_2$–pyridine, pyridine and $Mo_3S_8H_2$ systems are presented in Table 3, where we have shown properties for only one symmetry equivalent atom. As in the previous section, only relevant interactions are displayed. From the analysis of Table 3 the following features are worth to mentioning:

(i) As in the case of non-hydrogenated surface, the most important pyridine interactions occur with the Mo_1 atom but the bonding is weaker than in the previous case [24], see values in bracket. Nitrogen and C_3 atoms in the pyridine interact with two metallic centers giving rise to a more activated C–N bonds than in the case of structure I.

(ii) Two very important interactions N–H_6 and C_3–H_7 lead to bond formation (MBO (N–H_6) = 0.707, MBO (C_3–H_7) = 0.779, DE (N–H_6) = −0.598 au and DE (C_3–H_7) = −0.657 au) and are stronger than in case of system I. These strong interactions suggest that hydrogen atoms can be transferred from a hydrogenated MoS_2 surface to the pyridine molecule adsorbed on the Mo_1 site. This is also justified by the weakening of the H_s bonds of about a 50% (see values of MBO and DE for Mo_1–H_6, Mo_1–H_7, Mo_3–H_7 and Mo_2–H_6 bonds) with respect to the system without pyridine interaction.

(iii) An important agostic interaction between the H_3 of pyridine and the adjacent Mo atom (Mo_3...H_3–C_3) leads to a partial formation of the Mo_3...H_3 bond and a weakening of the H_3–C_3 one. This interaction, although is smaller that in the case of non-hydrogenated surface, also favors the formation of C_3–H_7 bond.

(iv) The interaction pyridine–$Mo_3S_8H_2$ produces also a weakening of the Mo_1–Mo_2 and Mo_1–Mo_3 bonds and a larger activation of the pyridine molecule than in the system I.

The above results for both π-adsorption systems (systems I and II) show that a complete hydrogenation of pyridine may occur after chemisorption. The energy difference between systems I and II is very small (5 kcal/mol). It means that pyridine is able to rotate on the Mo_1 center and hydrogenation and hydrogenolysis may happen by several steps: for example, a first step would be the hydrogenation of N and C_3 in system II (the highest H_6–and H_7–pyridine interactions, see values of H_6–N and H_7–C_3 in Table 3) with the formation of a diene-type intermediate. Initially the pyridine is adsorbed in the η^6 mode and after the first hydrogenation a η^4 coordination is expected. In a second step, after rotations of 60 and 120°, further hydrogenations would occur. These rotamers would be equivalent to II system, in the sense that H_6–and H_7–pyridine interactions with the not hydrogenated carbons (C_1, C_4 or C_2, C_5) are the highest. Note that in these conformations a radical intermediate is formed. A rotation of 90° also may occur, resulting in bonds C_1–C_5 and C_2–C_4 perpendicular to the row of Mo atoms, similar to system I. In this situation one may consider the chemisorption of two H_s atom on Mo_3 or Mo_2 sites, because Mo atoms of the clean surface present double unsaturation. Thus, a simultaneous

double hydrogenation of, for example, the C_2–C_4 bond may occur without having a radical intermediate. Another possibility could be the formation of a η^2 complex that can be hydrogenated by neighboring surface hydrogens. More work must be performed in order to have a complete mechanistic picture of this process.

The analysis of the interaction between the model surface $Mo_3S_8H_2$ and pyridine, for systems I and II shown in Fig. 2, suggests that the pyridine hydrogenation is a regioselective reaction. This result is in analogy with several homogeneous and heterogeneous systems [40,41], where the optimal orientation of the pyridine with respect to the catalyst surface determines the feasibility of the surface reaction. Fish et al. [42] suggested that the mode of bonding of the heterocyclic compounds to the metal centers of nickel oxide/aluminate supported on silica–alumina catalyst appears to be pivotal for the selective hydrogenation of the nitrogen containing ring and the subsequent bond cleavage.

3.3. System III

The system III is less stable than others discussed above, as shown the total energy values (TE) in Fig. 2. It corresponds to the σ-mode adsorption of pyridine and to the interaction of the nitrogen lone-pair with the Mo_1 surface atom. Several trends can be inferred from the analysis of the most important MBOs and DEs presented in Table 4 for System III: (i) As expected, there is only one important bonding interaction pyridine–$Mo_3S_8H_2$: N–Mo_1 interaction was found to be the highest of all calculated MBOs and DEs (0.900 and 0.464 au, respectively) for pyridine–cluster interactions. (ii) The C–N bond activation is very small as compare with systems I and II. (iii) The possibility of hydrogen atom transfer from the $Mo_3S_8H_2$ surface to the pyridine molecule is not feasible, because of the small MBO and AE values. (iv) Very small changes in the Mo_1–Mo_3, Mo_1–Mo_2 and Mo_x–H_s ($x=1, 2, 3$ and $s=6, 7$) bond are observed as compare with the non-interacting system with pyridine, see values in parentheses.

Table 4
Bonding properties of the system III ($Mo_3S_8H_2$-C_5H_5N) shown in Fig. 2c. Values in parentheses correspond to isolated systems ($Mo_3S_8H_2$ and pyridine). Values in brackets represent Mo_3S_8 system with pyridine interactions. For atom labels, see Fig. 1

Bond	MBO	DE (au)
$Mo_3S_8H_2$–pyridine		
Mo_1–N	0.900 [0.900]	−0.464 [−0.478]
Mo_1–C_1, C_2	0.134 [0.151]	−0.074 [−0.082]
Mo_2–C_2, Mo_3–C_1	0.101	−0.063
Mo_2–H_2, Mo_3–H_1	0.178	−0.051
C_1–H_7, C_2–H_6	0.028	−0.005
Pyridine		
C_1, C_2–N	1.649 (1.691)	−1.291 (−1.348)
$Mo_3S_8H_2$		
Mo_1–H_6, H_7	0.568 (0.670)	−0.185 (−0.224)
Mo_2–H_6, Mo_3–H_7	0.749 (0.818)	−0.236 (−0.241)
Mo_1–Mo_2, Mo_3	0.761 (0.841)	−0.153 (−0.195)

3.4. Charge transference

The population analysis performed in this CNDO method is Mulliken-type, and is well known that it presents serious deficiency [43]. Nevertheless, the charge difference between similar systems may be more reliable because of error cancelation. Thus, the results of charge transfer were considered here, i.e. the difference between atomic charges in pyridine–$Mo_3S_8H_2$ and the isolated pyridine and $Mo_3S_8H_2$. Several features come out from the analysis of results showed in Table 5:

(a) There is a clear indication that an electronic charge transfer from the pyridine to the Mo centers occurs, in all systems.

(b) The adsorbed hydrogens (H_s) are positively charged. This suggests that the surface hydrogens have an acidic character.

(c) The charge transfer from the pyridine to the Mo sites increases with the stability of the pyridine–$Mo_3S_8H_2$ system: I > II > III.

Table 5
Charges transferred due to the interaction of $Mo_3S_8H_2$ cluster with pyridine. Charge values were evaluated with respect to isolated systems

Atom	System I	System II	System III
Pyridine atoms			
N	+0.038	+0.115	+0.169
C_1	+0.122	+0.074	+0.047
C_2	+0.122	+0.074	+0.047
C_3	−0.008	+0.074	+0.029
C_4	+0.143	+0.094	+0.015
C_5	+0.143	+0.094	+0.015
Adsorbed hydrogens			
H_6	+0.119	+0.115	+0.003
H_7	+0.119	+0.053	+0.003
Molybdenum atoms			
Mo_1	−0.211	−0.094	−0.064
Mo_2	−0.236	−0.178	−0.132
Mo_3	−0.236	−0.239	−0.132

4. Conclusions

(a) Hydrogen adsorption on MoS_2 is favored at the bridge sites. Pyridine adsorption on a hydrogenated modeled surface of MoS_2 occurs mainly in the π-coordinated mode, Fig. 2a and 2b.

(b) Formation of H_s–pyridine ($s=6, 7$) bond is feasible in π-adsorption, particularly for the system II.

(c) There is a poor direct d-orbital participation in the interaction of Mo atoms with pyridine.

(d) The chemisorption of pyridine produces a weakening of Mo–Mo and Mo–H_s bonds.

(e) A mechanism for pyridine hydrogenation is proposed with the following steps: (i) adsorption of pyridine in π-coordination mode; (ii) hydrogenation of N and C atoms with the formation of a diene intermediate; and (iii) rotations of the pyridine molecule in order to hydrogenated other carbon atoms.

Acknowledgements

One the authors (ENR-A), acknowledges Decanato de Investigaciones y Desarrollo (USB) for Grant DI-CB-79-94 and CONICIT for Grant S1-2673. We thank the Laboratorio de Computación (USB) for a generous time grant on a Sun SPARC-2 workstation and Dr. Juan Rivero for helpful discussions.

References

[1] (a) J.R. Katzer and R. Sivasubramanian, Catal. Rev.-Sci. Eng., 20 (1979) 155. (b) R.N. Laine, Catal. Rev.-Sci. Eng., 25 (1983) 459. (c) R.N. Laine, New. J. Chem., 11 (1987) 543. (d) H. Schulz, M. Schon and N.M. Rahman, Stud. Surf. Sci. Catal., 27 (1986) 201. (e) T.C. Ho, Catal. Rev.-Sci. Eng., 30(1) (1988) 117. (f) G. Perot, Catal. Today, 10 (1991) 447. (g) S. Kasztelan, T. des Courières and M. Breysse, Catal. Today, 10 (1991) 433. (h) W. Böhringer and H. Schulz, Bull. Soc. Chim. Belg., 100 (1991) 831. (i) S. Eijsbouts, C. Sudhakar, V.H.J. de Beer and R. Prins, J. Catal., 127 (1991) 605. (j) E. Baralt, S.J. Smith, J. Hurwitz, I.T. Horváth and R.H. Fish, J. Am. Chem. Soc., 114 (1992) 5187.

[2] (a) C.N. Satterfield, M. Modell, R.A. Hites and C.J. Decbeck, Ind. Eng. Chem. Process. Des. Dev., 17 (1978) 141. (b) N. Nelson and R.B. Levy, J. Catal., 58 (1979) 485. (c) M.J. Ledoux, G. Agostini, R. Benazous and O. Michaux, Bull. Soc. Chim. Belg., 93 (8–9) (1984) 635. (d) M. Breysse et al., Bull. Soc. Chim. Belg., 96 (11–12) (1987) 829. (e) E. Hillerová and M. Zdrazil, Collect. Czech. Chem. Commun., 54 (1989) 2648. (f) M.J. Ledoux and B. Djellouli., J. Catal., 115 (1989) 580. (g) M.J. Ledoux and B. Djellouli., Appl. Catal., 67 (1990) 81. (h) E. Hillerová, M. Zdrazil and Z. Nit, Appl. Catal., 67 (1991) 231.

[3] B.C. Gates, J.R. Katzer and G.C.A. Schuit, Chemistry of Catalytic Processes, Mc Graw Hill, New York, 1979, p. 390.

[4] F.E. Massoth, Adv. Catal., 27(1978) 265.

[5] (a) J. Sonnemans, G.H. Van den Berg and P. Mars, J. Catal., 31 (1973) 220. (b) C.N. Satterfield and S. Gultekin, Ind. Eng. Chem. Process. Des. Dev., 20 (1981) 62. (c) M. Nagai, T. Masunaga and N. Hana-oka, J. Catal., 101 (1986) 284. (d) Z. Sarbak, React. Kinet. Catal. Lett., 32 (1986) 284. (e) K. Malakani, P. Magnoux and G. Perot, Appl. Catal., 30 (1987) 371.

[6] C.N. Satterfield, M. Modell and J.A. Wilkins, Ind. Eng. Chem. Process. Des. Dev., 19 (1980) 154.

[7] H.G. McIlvried, Ind. Eng. Chem. Process. Des. Dev., 10 (1971) 125.

[8] (a) M.A. Karolewski and R.G. Cavell, Surf. Sci. 210 (1989) 175. (b) F.P. Netzer and G. Rangelov, Surf. Sci., 225 (1990) 260. (c) M.R. Cohen and R.P. Merrill, Langmuir, 6 (1990) 1282. (d) C.N. Satterfield and J.F. Cocchetto, AIChE J., 21 (1975) 1107. (e) A. Kherbeche, R. Hubaut, J.P. Bonnelle and J. Grimblot, J. Catal., 131 (1991) 204.

[9] M.E. Bridge, M. Connolly, D.R. Lloyd, J. Somers, P. Jakob and D. Menzel, Spectrochim. Acta A, 43 (1987) 1473.

[10] B.J. Bandy, D.R. Lloyd and N.V. Richardson, Surf. Sci. 89 (1979) 344.

[11] N.V. Richardson, Vacuum, 33 (1983) 767.

[12] M. Connolly, J. Somers, M.E. Bridge and D.R. Lloyd, Surf. Sci., 185 (1987) 559.
[13] A.L. Johnson, E.L. Muetterties and J. Stöhr, J. Am. Chem. Soc., 105 (1983) 7183.
[14] J.U. Mack, E. Bertel and F.P. Netzer, Surf. Sci., 159 (1985) 265.
[15] J.E. Demuth, K. Christmann and P.N. Sanda, Chem. Phys. Lett., 76 (1980) 201.
[16] M. Bader, J. Haase, K.-H. Frank, A. Puschmann and A. Otto, Phys. Rev. Lett., 56 (1986) 1921.
[17] N.J. Di Nardo, Ph. Avouris and J.E. Demuth, J. Chem. Phys., 81 (1984) 2169.
[18] A.L. Johnson, E.L. Muetterties, J. Stöhr and F. Sette, J. Phys. Chem., 89 (1985) 4071.
[19] V.H. Grassian and E.L. Muetterties, J. Phys. Chem., 90 (1986) 5900.
[20] F.P. Netzer and J.U. Mack, Chem. Phys. Lett. 95 (1983) 492.
[21] F.P. Netzer and J.U. Mack, J. Chem. Phys., 79 (1983) 1017.
[22] F.P. Netzer, G. Rangelov, G. Rosina and H.B. Saalfeld, J. Chem. Phys., 89 (1988) 3331.
[23] P. Jakob, D.R. Lloyd and D. Menzel, J. Electron Spectrosc. Relat. Phenom., 44 (1987) 131.
[24] A.E. Gainza, E.N. Rodríguez-Arias and F. Ruette, J. Mol. Catal., 85 (1993) 345.
[25] I. Mayer and M. Révèsz, Comput. Chem., 6 (1982) 153.
[26] (a) A.J. Hernández, F. Ruette and E.V. Ludeña, J. Mol. Catal., 39 (1987) 21. (b) H. Castejón, A.J. Hernández and F. Ruette, J. Phys. Chem., 92 (1988) 4970.
[27] J.A. Pople and D.L. Beveridge, Approximate Molecular Orbital Theory, McGraw-Hill, New York, 1970.
[28] D. Rinaldi, GEOMO Program, QCPE, No. 290, 1976; D. Rinaldi, Comp. Chem., 1 (1976) 109.
[29] (a) F. Ruette, N. Valencia and R.A. Sánchez-Delgado, J. Am. Chem. Soc., 111 (1989) 40. (b) R. Atencio, L. Rincón, R. Sánchez-Delgado and F. Ruette, in preparation.
[30] R.G. Dickinson and L. Pauling, J. Am. Chem. Soc., 44 (1923) 1446.
[31] J.E. Del Bene, J. Am. Chem. Soc., 101 (1979) 7146.
[32] M. Sánchez and F. Ruette, J. Mol. Struct. (THEOCHEM), 254 (1992) 335, and references therein.
[33] (a) S. Siegel, J. Catal., 30 (1973) 139. (b) S. Kasztelan, H. Toulhoat, J. Grimblot and J.P. Bonnelle, Appl. Catal., 13 (1984) 127. (c) K.-I. Tanaka, Adv. Catal., 33 (1985) 99. (d) A. Wambeke, L. Jalowiecki, S. Kasztelan, J. Grimblot and J.P. Bonnelle, J. Catal., 109 (1988) 320. (e) Y. Okamoto, A. Maezawa and T. Imanaka, J. Catal., 120 (1989) 29. (f) J. Polz, H. Zeilinger, B. Müller and H. Knözinger, J. Catal., 120 (1989) 22. (g) S. Kasztelan, Langmuir, 6 (1990) 590. (h) S. Kasztelan, A. Wambeke, L. Jalowiecki, J. Grimblot and J.P. Bonnelle, J. Catal., 124 (1990) 12. (i) F.E. Massoth and P. Zeuthen, J. Catal., 145 (1994) 216. (j) T. Okuhara, H. Itho, K. Miyahara and K.-I. Tanaka, J. Phys. Chem., 82, 1978, 678.
[34] (a) A. Müller, Polyhedron, 5 (1986) 323. (b) A. Müller, E. Diemann, A. Branding, F.W. Baumann, M. Breysse and M. Vrinat, Appl. Catal., 62 (1990) L13. (c) E. Diemann, Th. Weber and A. Müller, J. Catal., 148 (1994) 288. (d) T.F. Hayden and J.A. Dumesic, J. Catal., 103 (1987) 366.
[35] A.J. Schultz, K.J. Stearly, J.M. Williams, R Mink and G.D. Stucky, Inorg. Chem., 16 (1977) 3303.
[36] J.E. Huheey, Inorganic Chemistry, Harper-Row Publishers, New York, 1978, p.842.
[37] A.B. Anderson, Z.Y. Al-Saigh and W.K. Hall, J. Phys. Chem., 92 (1988) 803.
[38] (a) R.L. Richards and C. Shortman, J. Organomet. Chem., 286 (1985) C3. (b) R.A. Henderson, D.L. Hughes, R.L. Richards and C. Shortman, J. Chem. Soc., Dalton Trans., (1987) 1115. (c) N.J. Lazarowich and R.H. Morris, J. Chem. Soc., Chem. Commun., (1987) 1865. (d) T.E. Burrow, N.J. Lazarowich, R.H. Morris, J. Lane and R.L. Richards, Polyhedron, 8 (1989) 1701. (e) T.E. Burrow, A. Hills, D.L. Hughes, J.D. Lane, N.J. Lazarowich, M.J. Maguire, R.H. Morris and R.L. Richards, J. Chem. Soc., Chem. Commun., (1990) 1757.
[39] M. Karplus and R.N. Porter, Atoms and Molecules, W.A. Benjamin, Inc., Menlo Park, CA, 1970, p. 202.
[40] R.H. Fish, H.-S. Kim, J.E. Babin and R.A. Adams, Organometallics, 7 (1988) 2250.
[41] (a) R.H. Fish, H.-S. Kim and R.H. Fong, Organometallics, 8 (1989) 1375. (b) R.H. Fish, H.-S. Kim and R.H. Fong, Organometallics, 10 (1991) 770. (c) R.H. Fish, E. Baralt and H.-S. Kim Organometallics, 10 (1991) 1965.
[42] R.H. Fish, J.M. Michaels, R.S. Moore and H. Heinemann, J. Catal., 123 (1990) 74.
[43] (a) S. Fliszár, Charge Distributions and Chemical Effects, Springer-Verlag, New York, 1983. (b) A. Sierraalta and F. Ruette, J. Comp. Chem., 15 (1994) 313.